Q-33

ANALYSIS OF MULTIPLE-STEP RADIAL-RESONATOR WAVEGUIDE DIODE MOUNTS WITH APPLICATION TO IMPATT OSCILLATOR CIRCUITS

Bevan D. Bates

Department of Electrical and Electronic Engineering
The University of Melbourne, Parkville, Victoria 3052, Australia

ABSTRACT

A computer-oriented method for determining the driving-point impedance of waveguide diode mounting structures incorporating stepped radial resonators is described. Results of application of the method to the study of IMPATT oscillator circuits are also given. The method is applicable to a wide range of diode mounts including the resonant-cap mount widely used in Gunn and IMPATT circuits.

INTRODUCTION

Radial-resonator diode mounts, such as the resonant-cap mount (1) have been in use for some time, particularly in IMPATT oscillators where a local low-loss resonator is desirable for impedance matching because of the low device impedance. Hitherto the design of such oscillators has been based largely either on experiment or on simplified analyses that do not include the effect of the waveguide boundary conditions, but assume a disc located above a ground plane in free space (2,3). Recently Bialkowski (4) has applied the image method of Williamson (5) to accurately account for the effect of the waveguide environment including either matched or short-circuited waveguide terminations. However, application to the method of Bialkowski to more general mounting structures, such as those shown in Fig. 1, requires the formulation of magnetic and electric field equations in each region and matching coefficients at each boundary. This paper presents a systematic approach for analyzing more general diode mounts that is suited to computer-aided design.

MOUNT ANALYSIS

The analysis of a radial mount may be represented symbolically as shown in Fig. 2 where [A], [B] and [C] are matrices describing the multi-mode coupling of between radial sections I, II, III and IV while the radial sections are described by a multi-modal admittance matrix derived from radial transmission-line equations (6). The coupling-coefficient matrices are determined by mode-matching at the boundaries of radial regions using a method similar to that of MacPhie et al. (7,8) and Omar and Schünemann (9) for rectangular or parallel-plate waveguide but applied to radial discontinuities. Circular symmetry is assumed.

Region III represents the rectangular waveguide region which is transformed to an equivalent radial region using the results of Bialkowski (4) and Williamson (5). Although this region is not circularly symmetric, determination of the input admittance involves an integration which averages the field with respect to circular variations. Thus, to a good approximation the input admittance of the waveguide region for each mode can be replaced by an equivalent radial admittance which is independent of angle. Thus at radius r in region ℓ of height b_ℓ at distance y_ℓ above waveguide wall at y = 0, the magnetic and electric fields may be described by

$$H_\phi^\ell(r) = \sum_{n=0}^{N_\ell} h_n^\ell(r) \cos k_{yn}^\ell (y-y_\ell)$$

$$E_y^\ell(r) = \sum_{n=0}^{N_\ell} e_n^\ell(r) \cos k_{yn}^\ell (y-y_\ell)$$

where N_ℓ is the mode number of the highest-order mode in region ℓ, $h_n^\ell(r)$ and $e_n^\ell(r)$ are the (complex) magnetic and electric field amplitudes of the nth mode, $k_{yn}^\ell = \frac{n\pi}{b_\ell}$ is the mode eigenvalue in region ℓ, and the time dependence is assumed to be $e^{j\omega t}$. Continuity of H and E at $r = r_1$ (the boundary between regions I and II) requires

$$\int_{y_I}^{y_I+b_I} H_\phi^I(R) \cos k_{ym}^I (y-y_I)\, dy$$

$$= \int_{y_I}^{y_I+b_I} H_\phi^{II}(R) \cos k_{ym}^I (y-y_I)\, dy ,$$

and

$$\int_0^{b_{II}} E_y^{II}(R) \cos k_{ym}^{II}\, y\, dy$$

$$= \int_{y_I}^{y_I+b_I} E_y^I(R) \cos k_{ym}^{II}\, y\, dy ,$$

0149-645X/87/0000-0669$01.00 © 1987 IEEE

where $E_y^I = 0$ on the conducting boundary. If we define equivalent mode voltages v_n and currents i_n by

$$e_{yn}(r) = -\frac{\varepsilon_{on}}{b} v_n(r); \quad h_{\phi n}(r) = \frac{i_n(r)}{2\pi r}$$

where ε_{on} is Neumann's number, then we can express the continuity equations at $r = r_1$ in matrix form as

$$\mathbf{I}^I_{r_1} = [A]\, \mathbf{I}^{II}_{r_1} \; ; \quad \mathbf{V}^{II}_{r_1} = [A]^T \mathbf{V}^{II}_{r_1} .$$

where $\mathbf{I}^I_{r_1}$ is a vector with elements $i_n(r_1)$ etc., and $[A]^T$ denotes the transpose of [A]. Similarly at r_2

$$\mathbf{I}^{II}_{r_2} = [B]\, \mathbf{I}^{III}_{r_2} \; ; \qquad \mathbf{I}^{IV}_{r_2} = [C]\, \mathbf{I}^{III}_{r_2} \; ;$$

and

$$\mathbf{V}^{III}_{r_2} = [B]^T \mathbf{V}^{II}_{r_2} + [C]^T \mathbf{V}^{IV}_{r_2} .$$

Now at r_2, $\mathbf{I}^{III}$ and $\mathbf{V}^{III}$ are related by the radial admittance seen looking outward from r_2, i.e., $\mathbf{I}^{III}_{r_2} = [Y^{III}]\, \mathbf{V}^{III}_{r_2}$ where $[Y^{III}]$ is diagonal. The elements of $[Y^{III}]$ are determined as in (4). Hence

$$\mathbf{I}^{II}_{r_2} = [B]\,[Y^{III}]\,[B]^T \mathbf{V}^{II}_{r_2} + [B]\,[Y^{III}]\,[C]^T \mathbf{V}^{IV}_{r_2} .$$

Using radial transmission theory to relate $\mathbf{V}^I_{r_1}$ and $\mathbf{I}^I_{r_1}$ to $\mathbf{V}^I_{r_2}$ and $\mathbf{I}^I_{r_2}$ (and similarly in region IV where $\mathbf{V}^{IV}_{r_1} = 0$), a relation is found between $\mathbf{I}_{r_1}$ and $\mathbf{V}_{r_1}$. If the height of region I is small enough, the electric field is constant and thus only one mode is considered. Thus

$$Y_{in} = \frac{i_{r_1}}{v_{r_1}}$$

is the desired input admittance of the mount. Note that in this case the matrix [A] reduces to a linear array of gap coupling factors as defined by Eisenhart and Khan (11).

APPLICATION

The above analysis has been applied in the study of IMPATT oscillator circuits by using a nonlinear IMPATT diode circuit model to predict oscillation frequency and power output (12). Fig. 3 shows a plot of the impedance from 8 to 10 GHz of a particular mount configuration as seen by the diode through the diode package (10 mm diameter disc in X-band waveguide with short positioned various distances from diode). Oscillation points are found from the Kurokawa condition $Z_C + Z_D = 0$, i.e., from the intersection of the circuit locus Z_C with a plot of the negative of the diode impedance $-Z_D$. Fig. 3 shows these intersection points obtained as the short-circuit position is varied over approximately half a guide wavelength (from 27.5 mm to 43.5 mm). These intersection points are found from an optimization routine which seeks to minimize $|Z_C + Z_D|^2$ by varying frequency and diode voltage (12). Fig. 4 shows the resulting frequency and power output as a function of short-circuit position compared with experimental results. The agreement is excellent.

Small variations in the mount configuration have a considerable influence on oscillator behavior. For example, Fig. 5 shows the effect of introducing a small radial step in the region above the disc resonator. The effect is to reduce the coupling of the radial cavity to the waveguide load as demonstrated by the small influence of the short position and the lower output power. The impedance plot (Fig. 6) shows that the diode is presented with very low impedances approaching a short-circuit condition. This results in large RF amplitudes but little power is coupled out of the resonant cavity. This also explains the larger discrepancy between measured and calculated output power than in Fig. 4 because the diode model is less accurate at larger RF amplitudes and resistive losses in the cavity (which have been ignored in the analysis) become significant.

CONCLUSION

A method for analyzing a wide variety of waveguide diode mounts has been outlined. Because regions within the mount can be assigned an arbitrary dielectric constant, the method is applicable to the study of a range of dielectric waveguide circuits provided the loss is small. The method has application in the design of waveguide oscillators and other circuits using radial steps for impedance matching or filtering.

ACKNOWLEDGEMENTS

The author is grateful for the assistance of M. Bialkowski. This work was supported by the Australian Research Grants Scheme and the Australian Telecommunications and Electronics Research Board.

REFERENCES

(1) I. S. Groves and D. E. Lewis, "Resonant-Cap Structures for IMPATT Diodes, Electron. Lett., vol. 8, pp. 98-99, Feb. 1972.

(2) G. A. Swartz, Y. S. Chiang, C. P. Wen, and A. Gonzalez, "Performance of P-Type Epitaxial Silicon Millimeter-Wave IMPATT Diodes, IEEE Trans. Electron Devices, vol. ED-21, pp. 165-171, Feb. 1974.

(3) A. C. Derycke and G. Salmer, "Circuit Analysis and Design of Radial Pretuned Modules Used for Millimeter-Wave Oscillators," IEEE Trans. Microwave Theory Tech., vol. MTT-33, pp. 600-609, July 1985.

(4) M. E. Bialkowski, "Analysis of Disc-Type Resonator Mounts in Parallel Plate and Rectangular Waveguides," AEÜ, vol. 38, pp. 306-310, Sept./Oct. 1984.

(5) A. G. Williamson, "Analysis and Modelling of a Single-Post Waveguide Mounting Structure," IEEE Proc. Pt H, vol. 129, pp. 271-277.

(6) M. B. Steer and P. J. Khan, "Wideband Equivalent Circuits for Radial Transmission Lines," IEEE Proc., vol. 128, Pt. H, pp. 111-113, April 1981.

(7) R. Safavi-Naini and R. H. MacPhie, "On Solving Waveguide Junction Scattering Problems by the Conservation of Complex Power Technique," IEEE Trans. Microwave Theory Tech., vol. MTT-29, pp. 337-343, April 1981.

(8) R. R. Mansour and R. H. MacPhie, "Scattering at an N-Furcated Parallel-Plate Waveguide Junction," IEEE Trans. Microwave Theory Tech., vol. MTT-33, pp. 830-835, Sept. 1985.

(9) A. S. Omar and K. Schünemann, "Transmission Matrix Representation of Finline Discontinuities," IEEE Trans. Microwave Theory Tech., vol. MTT-33, pp. 765-770, Sept. 1985.

(10) A. K. Talwar, "A Dual-Diode, 73 GHz Gunn Oscillator," IEEE Trans. Microwave Theory Tech., vol. MTT-27, no. 5, pp. 510-512, May 1979.

(11) R. L. Eisenhart and P. J. Khan, "Theoretical and Experimental Analysis of a Waveguide Mounting Structure," IEEE Trans. Microwave Theory Tech., vol. MTT-19, pp. 706-719, Aug. 1971.

(12) B. D. Bates and P. J. Khan, "Analysis of Waveguide IMPATT Oscillator Circuits," 1981 IEEE/MTT-S Int. Microwave Symp. Digest, pp. 232-234, Los Angeles, CA, June 1981.

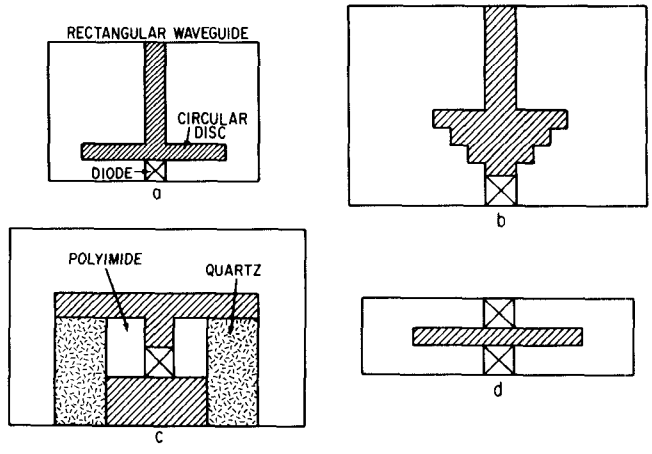

Figure 1. Radial-resonator waveguide diode mounts: (a) resonant-cap mount; (b) multiple-step mount; (c) pre-tuned module; (d) Talwar power combiner (10).

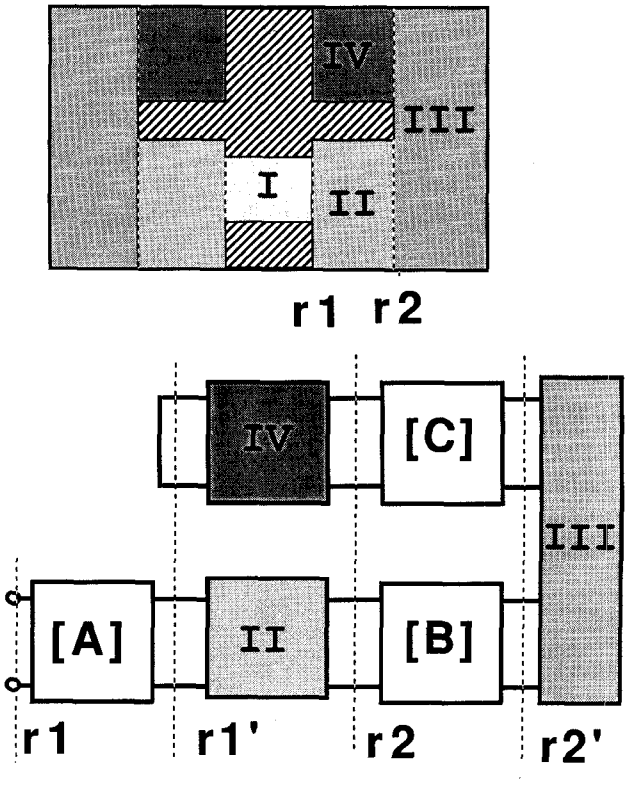

Figure 2. Block diagram representation of resonant-cap mount analysis.

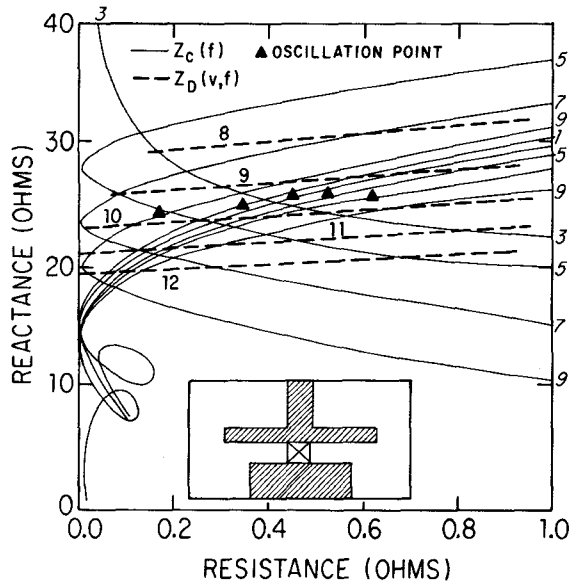

Figure 3. Mount impedance (including diode package) as a function of frequency for various short-circuit positions (1: 27.5mm, 3: 31.5mm, 5: 35.5mm, 7: 39.5mm, 9: 43.5mm). Also shown is negative of the diode impedance (dotted line) as a function of amplitude for various frequencies (8, 9, 10, 11, 12 GHz). Intersection of mount impedance and negative of diode impedance loci gives the oscillation points shown by ▲.

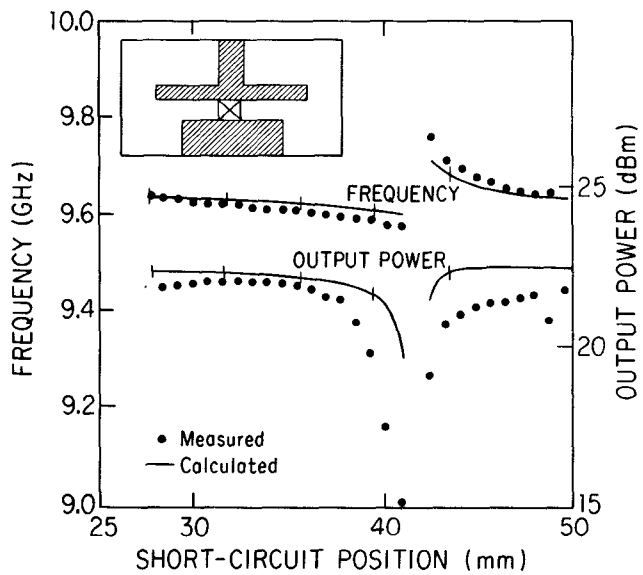

Figure 4. Comparison of measured and calculated frequency and output power as a function of short-circuit position for the mount shown (inset). Diode is MA-46022 IMPATT biased at 50 mA.

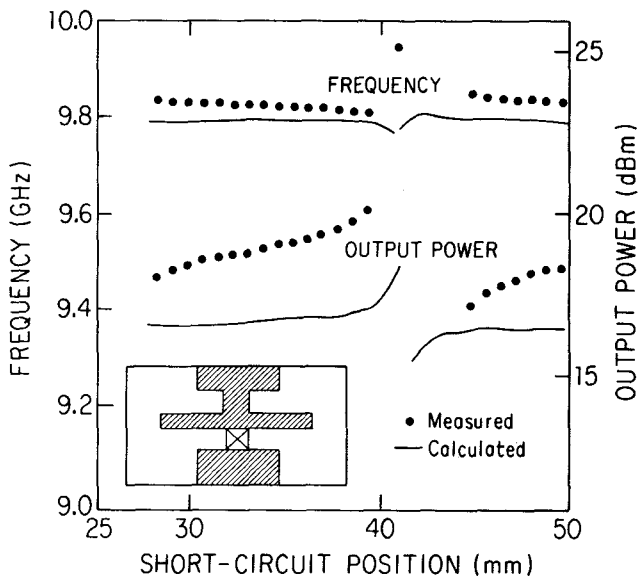

Figure 5. Comparison of measured and output power as a function of short-circuit position for mount configuration shown.

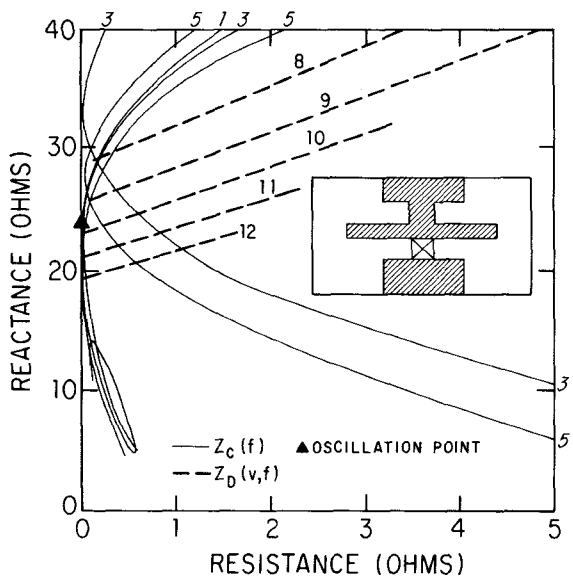

Figure 6. Impedance plot for mount shown. Legend for curves is in Fig. 3.